

# GCN-Geo: A Graph Convolution Network-based Fine-grained IP Geolocation System

Shichang Ding, Xiangyang Luo\*, Jinwei Wang, *Member, IEEE*, and Neal Naixue Xiong, *Senior Member, IEEE*

**Abstract**—Fine-grained IP geolocation systems often rely on some linear delay-distance rules. They are not easy to generalize in computer network environments where the delay-distance relationship is non-linear. To improve the generalization capabilities, researchers begin to pay attention to deep learning-based IP geolocation systems recently. These data-driven systems leverage multi-layer perceptron (MLP) to model non-linear relationships. However, MLP is not so suitable for modeling computer networks because networks are fundamentally graph-structured data. MLP-based IP geolocation systems only treat IP addresses as isolated data instances, forgoing the connection information between IP addresses. This would lead to suboptimal representations of computer networks and limit the geolocation performance.

Graph convolutional network (GCN) is an emerging deep learning method for graph-structured data presentation. However, limited attention has been paid to introducing GCN into IP geolocation problem. In this work, we research how to model computer networks for fine-grained IP geolocation with GCN. First, we formulate the IP geolocation task as an attributed graph node regression problem. Then, a GCN-based IP geolocation system named GCN-Geo is proposed to predict the location of each IP address. GCN-Geo consists of a preprocessor, an encoder, graph convolutional (GC) layers and a decoder. The preprocessor and the encoder transform raw network measurement data into the initial graph node & edge embeddings. GC layers can refine the initial graph node embeddings by explicitly modeling the connection (edge) information between IP addresses. The decoder maps the refined node embeddings to the geolocation of nodes (IP addresses). The proposed decoder can relieve the converging problem of GCN-Geo by considering the prior knowledge, which is about the coarse-grained location of target IP addresses. Finally, the experimental results in three real-world datasets (New York State, Hong Kong, and Shanghai) show that: (i) the best baselines are all different in the three datasets because the generalization capabilities of baselines are limited; (ii) GCN-Geo clearly outperforms the state-of-art rule-based and learning-based baselines on all three datasets on average error distance, median error distance and max error distance. For example, compared with the best baselines in each dataset, GCN-Geo can reduce the average error distance by 16% to 28%. The parameter studies also reveal the configurations which could significantly influence the performance of GCN-Geo, such as aggregation

methods. This work verifies the great potential of GCN in fine-grained IP geolocation.

**Index Terms**—Fine-grained IP Geolocation Systems, Graph Convolutional Network, Computer Network, Deep Learning

## 1. INTRODUCTION

IP geolocation technology aims to obtain the geographic location of a given IP address [1, 2]. It has been widely used in localized online advertisement, location-based content restriction, cyber-crime tracking, and so on [1, 3]. IP geolocation service is important especially when internet users are using equipments without GPS (Global Positioning System) function, such as PCs and routers. Accuracy is one of the most important performance objectives for IP geolocation service. Existing IP geolocation systems can be categorized into two kinds by accuracy: coarse-grained IP geolocation and fine-grained IP geolocation.

Coarse-grained IP geolocation can find the city or state location of an IP address. Researchers have proposed a series of coarse-grained IP systems such as [1, 3]. Commercial databases can also be used to provide a coarse-grained location of IP addresses [1, 4]. The median error distances of these systems are between dozens and several hundreds of kilometers. After obtaining a coarse-grained location of a target IP, fine-grained IP geolocation systems can be used to find its more accurate location. The median error distances of fine-grained IP geolocation systems are usually around or less than 10 kilometers. Though there are several fine-grained IP geolocation systems like SLG [5], Checkin-geo [6], MLP-Geo [7] and Corr-SLG [2], fine-grained IP geolocation stills faces many challenging problems [1], such as generalization capabilities in different network environments and reliable fine-grained landmarks<sup>1</sup>. **In this paper, we mainly focus on improving the generalization capabilities of measurement-based fine-grained IP geolocation.**

Measurement-based IP geolocation can geolocate a target IP after the probing host [2] obtains the measurement data (e.g., routing data) to the target IP and landmarks [2, 5]. Generally, existing measurement-based fine-grained IP geolocation systems can be categorized into two kinds: rule-based and deep learning-based systems.

For rule-based systems like SLG, [5] and Corr-SLG [2], they assume that most hosts in one network are following some delay-distance rules. Then they can map a target IP to its nearest landmark by transforming its delay to distance. For example, the rule of SLG is that the shortest "relative delay"

<sup>1</sup>Landmarks are IP addresses with known locations [2, 5]

This work has been submitted to the IEEE for possible publication. Copyright may be transferred without notice, after which this version may no longer be accessible. This work was supported by the National Natural Science Foundation of China (Grant No.U1804263, 61872448 and 62172435), and Zhongyuan Science and Technology Innovation Leading Talent Project of China (Grant No. 214200510019). (Corresponding author: Xiangyang Luo)

Shichang Ding and Xiangyang Luo are with State Key Laboratory of Mathematical Engineering and Advanced Computing, Zhengzhou 276800, China. email: scdingwork@outlook.com, luox\_y\_ieu@sina.com

Jinwei Wang is with School of Computer and Software, Nanjing University of Information Science & Technology, Nanjing 210044, China. email: wjwei\_2004@163.com

Neal Naixue Xiong is with the Department of Mathematics and Computer Science at Northeastern State University, OK 74464, USA. email: xiong-naixue@gmail.com

comes from the nearest landmark [5]. However, this rule is not valid for all intra-city networks. For example, authors of Corr-SLG find that in some cities like Toronto (Canada) and Zhengzhou (China), the rule of SLG is not suitable for many hosts [2]. Corr-SLG improves SLG by dividing hosts into three groups according to their relative-delay-distance correlation. Corr-SLG applies the different linear delay-distance rules in different groups. Even so, Corr-SLG cannot accurately geolocate the hosts which follow non-linear delay-distance rules. Generally speaking, the performances of the rule-based systems rely on the partition of hosts which follow the pre-assumed linear delay-distance rules. However, distance is usually not the dominant effect for delay inside cities [2]. Therefore, the partition of hosts following the linear delay-distance rule could be low in many intra-city networks. This limits the generalization capabilities of rule-based systems.

Recently, deep learning seems to be a hopeful solution to the generalization problem of IP geolocation in different computer network environments. There are two possible advantages of deep learning-based (shorten as learning-based) IP geolocation systems. First, learning-based systems do not need strong pre-assumptions of delay-distance rules. These data-driven models can learn specific delay-distance (or routing-distance) relationships based on the raw measurement data of each computer network. Second, learning-based systems are capable of extracting non-linear relationships, while non-linear rules are hard for human experts to recognize. Encouraged by the possible advantages, researchers proposed several IP geolocation systems based on deep learning, such as NN-Geo [8] and MLP-Geo [7]. These systems use MLP (multi-layer perceptron) to learn the relationship between the measurement data (e.g., delay and routing information) and the targets' locations. Among them, MLP-Geo is a fine-grained IP geolocation system.

However, the generalization ability of MLP-Geo is still not satisfying. Based on our experiments (shown in Table I) in different actual networks, MLP-Geo is not always better than rule-based systems such as [2, 5]. This is because MLP is still not the ideal learning-based method for modeling computer networks. MLP is good at preprocessing Euclidean structure data, while the computer networks are fundamentally graph-structured data (a typical non-Euclidean structure data) [9, 10]. Limited by the design of MLP, it is hard for MLP to model the connection information of the network. MLP-based IP geolocation systems can only treat the IP addresses as independent instances. However, hosts in one network are non-independent and linked to each other by intermediate routers. Both NN-Geo and MLP-Geo only leverage the direct delay between the probing host and the targets, ignoring all the other useful features, such as delays between routers and the IP addresses of routers. Though MLP-Geo also leverages the routers' IDs between the probing host and targets, it still cannot learn the relationship between these routers, or the relationship between routers and targets. Therefore, MLP cannot fully describe the network topology. This could lead to suboptimum results since MLP lacks the ability to introduce more useful information into IP geolocation.

In recent years, Graph Convolutional Network (GCN)

emerges as one of the most advanced deep learning methods for graph data presentation [11]. It has achieved great success in different fields of graph data, like recommendation system [12], social network [13], knowledge map [14], chemistry [15], etc. However, little attention has been paid to utilizing GCN for fine-grained IP geolocation problems. As far as we know, we are the first to explore the potential of GCN in fine-grained IP geolocation.

The main challenges of introducing GCN into IP geolocation tasks are four-folds.

- 1) How to formulate IP geolocation problem in the context of graph deep learning?
- 2) Why GCN would outperform MLP in IP geolocation?
- 3) How to design a proper GCN-based system for the fine-grained measurement-based IP geolocation task?
- 4) Which factors will affect the performance of the GCN-based system for fine-grained IP geolocation?

By tackling these challenges, the main contributions of our work can be summarized as follows.

- 1) We formulate the measurement-based fine-grained IP location problem as a semi-supervised attributed-graph node-level regression problem. First, IP addresses are mapped into graph nodes, and links are mapped into graph edges. Then, the features of IP addresses (e.g, delay) and links (e.g, the delay of link) can be naturally transformed into attributes of the graph nodes and edges. Finally, the IP geolocation problem is formulated as estimating the latitudes and longitudes of the target graph nodes based on the known locations of other graph nodes.
- 2) By analyzing the difference in forming the embeddings of IP addresses, we explain the advantages of GCN-based IP geolocation systems compared to MLP-based IP geolocation systems.
- 3) We propose a GCN-based system to solve the node regression problem, which is called GCN-Geo. It consists of four components: a preprocessor, an encoder, GC (graph convolutional) layers, and a decoder. The preprocessor transforms the raw traceroute data of a computer network into an attributed-graph representation. The encoder generates the initial graph node/edge embeddings for GC layers. The GC layers refine the node embeddings by propagating messages along the edges. Finally, the latitudes and longitudes of each node can be decoded from the refined node embeddings.
- 4) We highlight the limitation of the general decoder, which makes the GCN-based IP geolocation systems hard to converge. We relieve the converging problem with a rule-based decoder. The core idea of the rule-based decoder is making GCN-Geo find targets' fine-grained locations inside a possible coarse-grained area. The experiments show that the rule-based decoder can significantly reduce the error distance and training epoch numbers of GCN-based IP geolocation systems.
- 5) The geolocation experiments are carried out in three real-world networks including New York State, Hong Kong, and Shanghai. The best baselines are different

in three datasets w.r.t. different metrics. In all three networks, the GCN-Geo system clearly outperforms the rule-based and learning-based systems on average error distance, median error distance, and max error distance. For example, compared with the best baselines in each dataset, GCN-Geo reduces the average error distances by 16% to 28%. The parameter studies show that parameters like aggregation methods and the depth of GC layers can clearly affect the performance of GCN-Geo. These empirical results validate the potential of GCN in fine-grained IP geolocation.

The rest of the paper is organized as follows. In Section 2, we introduce the related works of fine-grained IP geolocation as well as the applications of GCN in computer networks. In Section 3-A, IP geolocation is formulated into an attributed graph node regression problem. In Section 3, with a discussion of the advantages of GCN compared to MLP in IP geolocation. In Section 4, we propose the GCN-Geo system. Section 5 shows and analyzes the experiment results in three real-world datasets. Finally, the pros and cons of GCN-Geo are concluded in Section 6 with a short discussion of future works.

## 2. RELATED WORK

In this section, we introduce the works related to our study, mainly including fine-grained IP geolocation systems and the applications of Graph Convolution Network in computer networks.

### A. Fine-grained IP Geolocation

Besides measurement-based systems, there are two other kinds of fine-grained IP geolocation systems: database-based and data-mining-based system. IP geolocation databases can only provide the fine-grained locations for a small proportion of IP addresses, which could hardly satisfy people's needs [4]. Data-mining-based systems, like Checkin-Geo [6], can map IP addresses to locations based on a mass amount of raw data which contains "IP-location" information such as users' logs. However, these kinds of raw data resources are only possessed by few internet giants like Microsoft Bing [4] and Tencent [6], which are not open to the public. For example, Checkin-Geo is a data-mining-based fine-grained system. First, it extracts users' names and their locations from the checkin [6] information collected on smartphone applications. Then it extracts users' names and users' IP addresses from the logins collected on PC applications. In the end, Checkin-Geo can map a user's PC IP address to his/her smartphone location. Both the PC and the smartphone applications are owned by a famous Chinese online social platform called "Tencent QQ". These data resources are only open to researchers who work together with Tencent. Besides this problem, data-mining-based systems cannot work well in areas where those Internet giants are not serving, or the location-sharing service is forbidden. For example, Tencent QQ mainly serves in China and has been banned in India<sup>2</sup>.

The limitations of database-based and data-mining-based systems require researchers to pay attention to measurement-based systems. In theory, measurement-based systems can geolocate any target IP if the delay or routing data between the target IP address and landmarks can be obtained. However, it is hard for measurement-based systems to get a fine-grained geolocation result. Because the relationship between measurement data and target IP's location is very complicated and different in various network environments.

SLG is the first fine-grained measurement-based IP geolocation system [5]. It is also the first rule-based system as well as one of the most widely-used fine-grained IP geolocation baselines until now. It assumes that most hosts in a network are following a simple linear delay-distance rule: the shortest "relative delay" comes from the nearest landmark. Since the delay between a landmark and a target IP is hard to measure, "relative delay" is proposed by SLG as an approximation. Assume the delay from the probing host to a target IP is  $d_{pt}$ , the delay from the probing host to a landmark is  $d_{pl}$ , and the delay from the probing host to the closest common router [2, 5] shared by the target IP and landmark is  $d_{pr}$ , the "relative delay" between the target and the landmark is  $(d_{pt} - d_{pr}) + (d_{pl} - d_{pr})$ . This rule originated from an observation of the relationship between relative delay and distance of 13 landmarks in New York City [5]. However, in further studies, researchers realized that this rule may be not valid for all intra-city networks.

Researchers in Corr-SLG find that there is no clear relationship between relative delay and distance in Zhengzhou (China) and Toronto (Canada). They explain that for the intra-city delay, the delay caused by geographical distance are not always the major constituent. The other factors like queuing delay and processing delay in routers could be more important. Thus the relationship between relative delay and distance is very complicated. In Corr-SLG, the relative-delay-distance correlation of all landmarks is calculated at first. Then all landmarks are divided into three groups. Corr-SLG leverages different delay-distance rules in each group. In the groups with a strong-positive relative-delay-distance correlation (close to 1), the relative delay increases as the distance increases. Thus the rule is similar to SLG, and Corr-SLG still map targets to the landmarks with the shortest relative delay. In the groups with a strong-negative correlation, they map targets to the landmarks with the largest relative delay (close to -1). However, Corr-SLG cannot decide how to handle the groups with weak correlation (close to 0). They simply map these targets to the average locations of landmarks. We can see the accuracy of the rule-based systems relies on the partition of hosts which follows their pre-assumed rules. Since the network environments may change in each city and at different times, the performances of rule-based systems vary significantly. **How to design a fine-grained system that can well generalize in different networks is an important problem.**

In recent years, deep learning attract many researchers' attention [16–23]. People tried to utilize deep learning systems in IP geolocation to improve the generalization capabilities. Both NN-Geo [8] and MLP-Geo [7] use MLP to estimate locations for target IP addresses. Compared with NN-Geo,

<sup>2</sup>[www.xda-developers.com/india-bans-xiaomi-mi-browser-pro-qq-international-app/](http://www.xda-developers.com/india-bans-xiaomi-mi-browser-pro-qq-international-app/)

MLP-Geo adds a new kind of useful information – the routers' IDs between probing hosts and the targets. Its performance is much better than NN-Geo since NN-Geo only utilizes the delay between probing hosts and the target IP. The aim of learning-based systems is not to find a rule which is suitable for all networks. Instead, they aim to present a system which can correctly find "rules" in different networks. Whether a system can find rules correctly mainly relies on its modeling ability towards the target networks. Actually, MLP is not so suitable for modeling the measurement data of computer networks. MLP is good at preprocessing Euclidean structure data. However, the topology of the internet is a non-Euclidean structure data [24]. MLP can only treat target IP addresses as isolated data instances while forgoing the connection information between targets. This would easily lead to suboptimal representations and limit the performance. We still need to improve the learning-based systems by utilizing deep learning systems more suitable to networks.

### B. The Applications of GCN in Computer Networks

Graph Convolutional Network (GCN) is an emerging deep learning method, which is specially designed for graph-structured data in recent years [11, 15]. GCN can effectively capture the spatial information of the network topology. It is natural for researchers to try GCN in different problems of computer networks [24]. For example, network modeling is used to reconstruct the computer networks and predict the unseen computer networks. GCN has been introduced into network modelling in [25, 26]. [27, 28] discuss how to utilize GCN in network calculus analysis. GCN is also helpful in network delay prediction [29] and network traffic prediction [30–32]. GCN has been introduced into automatic detection for Botnets, which is important to prevent DDoS attacks[33]. However, little attention has been paid to IP geolocation as far as we know.

## 3. BASIC FINE-GRAINED IP GEOLOCATION SYSTEMS AND DEFINITIONS

### A. IP Geolocation Formulation

To explore the potential of GCN in fine-grained IP geolocation, we need to formulate IP geolocation as a graph-based learning problem at first. In this paper, the IP addresses  $IP_i, i = 1, 2, \dots, N_{IP}$  and the links  $LK_j, j = 1, 2, \dots, N_{LK}$  between IP addresses are used to represent the topology of a computer network. The link means a direct physical link between two IP addresses. The location of each IP address is represented as a pair of (latitude, longitude). Each IP address is associated with measured attributes, such as the delay from the probing host. Each link is also associated with measured attributes, such as the delay of the link. All IP addresses can be divided into four groups: the probing host IP address, the landmark IP addresses, the target IP addresses and the router IP addresses. The router IP addresses are the intermediate router IP addresses found by the probing host when tracing the landmarks and targets.

As shown in Fig. 1, we map a computer network topology to an attributed undirected graph,  $G = (V, E, XV, XE)$ . In

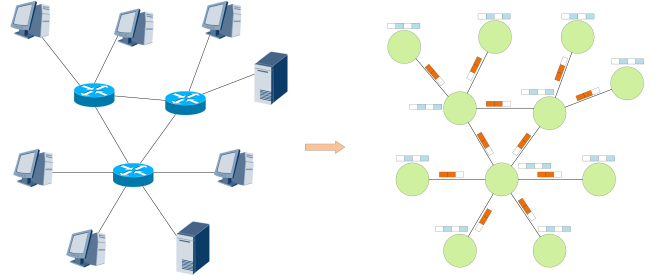


Fig. 1: Mapping a Computer Network into An Attributed Graph

the graph, a graph node  $v_i \in V, i \in \{0, 1, \dots, N_V\}$  represents an IP address  $IP_i$ . Each link  $LK_j$  is represented as a graph edge  $e_j \in E, j \in \{0, 1, \dots, N_E\}$ . Let  $xv_i \in XV, i \in \{0, 1, \dots, N_V\}$  and  $xe_j \in XE, j \in \{0, 1, \dots, N_E\}$  represent the attributes of the node  $v_i$  and the edge  $e_j$ , respectively. The latitude and longitude location of  $v_i$  are  $loc_{v_i}$ . The two dimensions of  $loc_{v_i}$  are  $[-90, 90]$  and  $[-180, 180]$ , respectively. Assume the node belongs to the probing host, landmarks, targets and routers are  $V_p, V_l, V_t$  and  $V_r$ . Then the locations of the probing host and landmarks are  $\{loc_{v_i}, v_i \in \{V_p, V_l\}\}$ . The locations of targets are  $\{loc_{v_i}, v_i \in V_t\}$ . Herein, the measurement-based IP geolocation problem is formulated to learn a prediction function  $f(\cdot)$ , which can estimate the targets' location:

$$\{\{loc_{v_i}, v_i \in \{V_p, V_l\}\}; G\} \xrightarrow{f(\cdot)} \{\widehat{loc_{v_i}}, v_i \in V_t\}, \quad (1)$$

where the outputs are targets' estimated locations  $\{\widehat{loc_{v_i}}, v_i \in V_t\}$ , and the inputs are (i) the attributed undirected graph  $G = (V, E, XV, XE)$ ; (ii) the known locations of the probing host and landmarks  $\{loc_{v_i}, v_i \in \{V_p, V_l\}\}$ . In this paper, we use the numerical values of (latitude, longitude) to represent the location of each node, thus this is an attributed graph node regression problem. If the location is categorical, like communities or streets, the IP geolocation problem can also be formulated into a node classification problem. Note that researchers usually do not have the location information of intermediate routers  $V_r$ , thus this is also a typical semi-supervised problem. It is worth reporting here, it is also easy to estimate the location of intermediate routers by formulating IP geolocation into a graph node regression problem. Because the graph representations of router nodes can be naturally learned along with target nodes.

### B. The Advantages of GCN-based Systems

Generally speaking, there are two key phases in deep learning-based IP geolocation systems: (i) target embedding and (ii) target location mapping. From previous measurement-based IP geolocation systems like [2, 5, 7], we know raw network measurement data contains useful signals which can help in IP geolocation. The target embedding phase is responsible to extract all useful signals from raw network measurement data, and then compress them into vectorized representations of target IP addresses (i.e., targets' embeddings). Then the target location mapping phase is responsible to map targets'

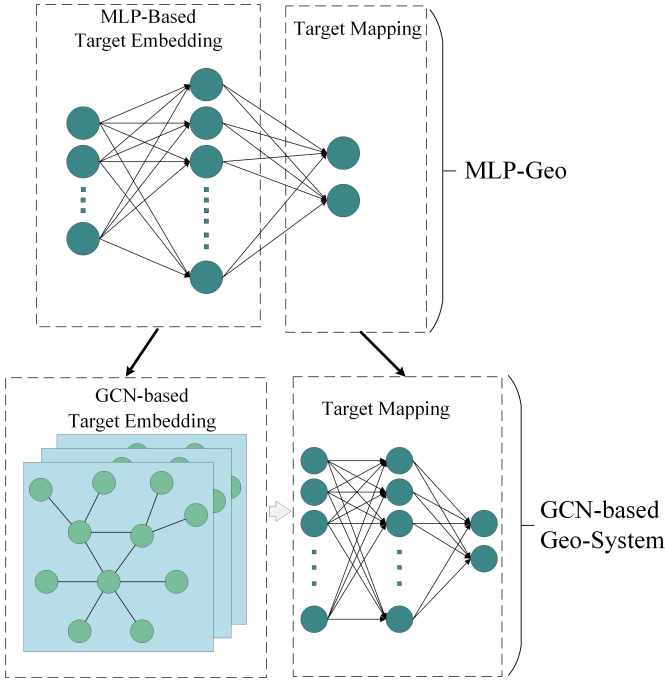


Fig. 2: The Difference between MLP-Geo and a Possible GCN-based IP Geolocation System

embeddings to targets' locations. The main problem of MLP-Geo is that its target embedding phase fails to extract many useful signals from measurement data.

In Fig. 2, we show previous learning-based system MLP-Geo and a possible GCN-based IP geolocation system. We mainly analyze the difference between their target embedding phase. As shown in Fig. 2, MLP-Geo consists of three dense layers. The first two dense layers or the first dense layer can be seen as its target embedding phase. Here we assume its target embedding phase consists of the first two layers. And the last dense layer is MLP-Geo's target location mapping phase. Then the targets' embeddings  $E_{mlp}^2$  of MLP-Geo are generated as follows:

$$E_{mlp}^2 = f_2(f_1(Input)), \quad (2)$$

$$f_i = \sigma(W_i X_i + b_i), \quad (3)$$

where  $Input$  is the input features of MLP-Geo,  $f_i$  denotes the  $i$ -th-dense-layer of MLP-Geo,  $W_i$  is the weight of the  $i$ -th-dense-layer, and  $b_i$  is the bias of the  $i$ -th-dense-layer.  $X_i$  is the input of  $i$ -th-dense-layer and the output of the  $(i-1)$ -th-dense-layer.  $Input$  is  $X_0$ . In MLP-Geo,  $Input$  consists of the delay and router IDs from the probing host to the targets. From Formula 3, we can see the dense layer  $f_i$  uses matrix multiplication to extract useful signals from the input data. In this way, it can only judge whether a router ID shows in the path between the probing host and a target. MLP-Geo cannot extract the sequence relationship of the routers between the probing host and targets. It also cannot describe the topology around an IP addresses (or the whole network). And it cannot leverage the delay between two directly-linked IP addresses, which have been proved useful by the rule-based systems like SLG. It also cannot consider the influence of the digits of IP

addresses. For example, 110.220.100.32 and 110.220.100.35 may belong to one organization and are near to each other. It is hard for MLP-Geo to extract these useful signals because it is not designed for non-Euclidean structure data like graph.

GCN is a deep learning method designed for graph-typed data [11, 15]. Its core concept is message passing. As we mentioned in Section 3-A, all IP addresses are transformed into graph nodes. As shown in Fig. 2, we use GCN as the target embedding phase to generate node embeddings as follows.

$$E_i^{gcn} = f_i(\dots(f_2(f_1(E_0))), \quad (4)$$

$$f_i = \{f_{message}, f_{aggregate}, f_{update}\}, \quad (5)$$

$$M_i = f_{message}(E_{i-1}^{neighbour}, E^{link}), \quad (6)$$

$$MS_i = f_{aggregate}(M_i), \quad (7)$$

$$E_i^{gcn} = f_{update}(MS_i, E_{i-1}^{gcn}), \quad (8)$$

where  $f_i$  indicates the  $i$ -th-GC-layer,  $E_i^{gcn}$  is the node embeddings of the  $i$ -GC-layer,  $E_0$  denotes the input (initial node embeddings). We can see both GCN and MLP learn new embeddings for IP addresses over multiple layers (since they are all deep learning methods). However, one GC layer  $f_i$  consists of three functions: the message function  $f_{message}$ , the aggregate function  $f_{aggregate}$  and the update function  $f_{update}$ . For a graph node, the message function  $f_{message}$  passes its neighbor node's embedding ( $E_{i-1}^{neighbour}$ ) along the edge/link ( $E^{link}$ ) to it. A neighbor node means there is one edge between these two nodes. Then the aggregate function  $f_{aggregate}$  collects the aggregation of all its neighbor nodes' messages ( $MS_i$ ). The update function  $f_{update}$  forms the node's new embedding  $E_i^{gcn}$  based on the aggregated messages  $MS_i$  and the node's previous embeddings  $E_{i-1}^{gcn}$ .

From Formula 4-8, we can see the embedding of each graph node also aggregates with neighbor nodes' embeddings and its edge embeddings at the beginning of each GC layer. And in  $i$ -th-GC-layer, a node can get information from its  $i$ -hop neighbors. For example, in the  $2rd$ -GC-layer, a node not only gets messages from its 1-hop neighbors, but also gets information from 2-hop neighbors. Because the messages from its 2-hop neighbors are passed to its 1-hop neighbors in  $1st$ -GC-layer. Through passing messages along the edges, after  $i$  GC layers ( $i$  is usually larger than 2), every node will gradually know the topology and node/edge attributes of the computer network. So compared with MLP, GCN can naturally describe the network topology in the targets' embeddings. And the other features like delay of links and IP addresses can also be utilized, because they can be easily combined into message function  $f_{message}$ , or the embeddings of links  $E^{link}$ . Thus GCN can extract more kinds of useful signals from measurement data than MLP during target embedding phase. Next we will introduce how to build a fine-grained IP geolocation system based on GCN in detail.

#### 4. OUR PROPOSED GCN-GEO SYSTEM

We present the GCN-Geo system in this section. Fig. 3 illustrates the system, which consists of four components: a preprocessor, an encoder, GC layers, and a decoder. The preprocessor maps the raw measurement data of a computer



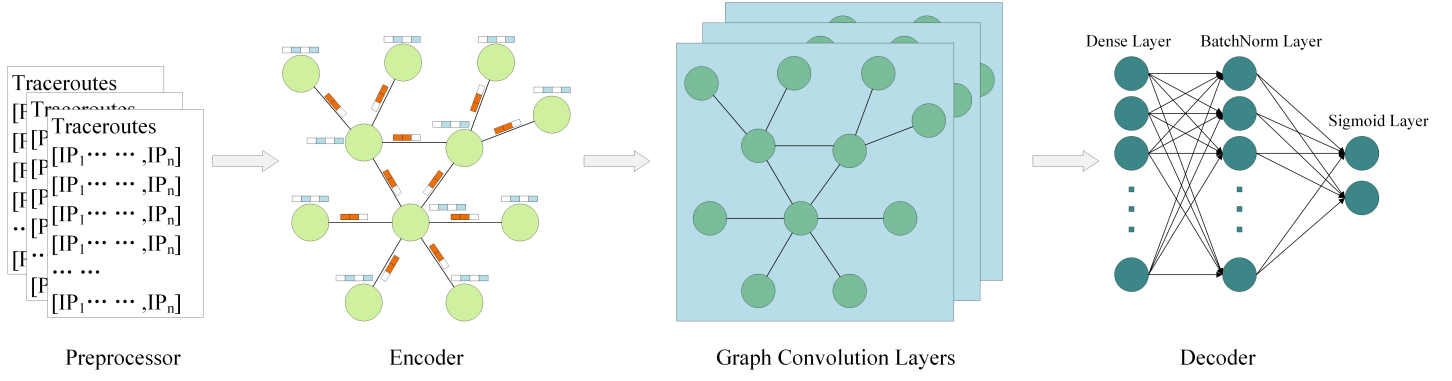


Fig. 3: Illustration of the GCN-Geo System

network into its graph representation  $G = (V, E, XV, XE)$ . The encoder generates the initial feature embeddings of  $G$ . The GC layers refine the initial feature embeddings with graph signals and output the refined embeddings for all nodes  $V$ . Finally, the decoder maps the refined node embeddings into the locations. We will describe each component one by one, followed by the optimization details.

#### A. The Preprocessor

In this paper, the measurement data is mainly traceroute data from the probing host to landmarks and targets. The task of the preprocessor is transforming the raw traceroute data into the initial embeddings of  $G = (V, E, XV, XE)$  for the encoder. This mainly consists of two sub-tasks: (i) building the Graph  $G$  with the graph nodes  $V$  and the links  $E$ ; (ii) extracting the node attributes  $XV$  and the link attributes  $XE$ .

1) *Building Graph: Node*. As mentioned in Section 3-A, we use the IP addresses and the links between IP addresses to represent the topology of a computer network. Thus all IP addresses in the raw traceroute data are transformed into the graph nodes. Each node  $v_i$  is differentiated by a node ID. The ID is from 1 to  $N_V$ .  $N_V$  is the number of all IP addresses found in traceroute data.

**Edge**. If the probing host finds a direct physical link between two IP addresses, then the link is transformed into a graph edge  $e_j$ . During the traceroute, it is possible that the probing host cannot get the IP address and delay of some routers, which are called "anonymous routers". There are two kinds of systems to build an edge over "anonymous routers": (i) ignore anonymous routers and build an edge between the two routers before and after the anonymous routers along the routing path; (ii) map anonymous routers to IP addresses found in other re-measured routing paths. Both solutions are tested in early experiments. The difference in their final geolocation performances is not significant. This may be due to that GCN itself is a powerful feature extractor, which is not sensitive to such differences in the input graph. However, the first solution introduces more edges in  $G$ , which leads to higher computation complexity and greater memory needs in the optimization phase. Thus we leverage the second solution in this paper, which is introduced as follows.

After tracing one IP address multiple times, we may get

several different routing paths. We assume that if two routing paths are the same as each other except for the anonymous routers, then the two paths are likely to be similar. Then we can map the anonymous routers in one path to the IP addresses in other similar paths. Our matching algorithm is shown in Algorithm 1. The raw path set refers to all the raw paths found by the traceroute. The completed path set refers to the paths of which the anonymous routers have been mapped to IP as much as possible. After using Algorithm 1, we can build edges based on the completed paths. We ignore any anonymous routers which are still not mapped to IP addresses. And then an edge is built between the two routers before and after the anonymous routers along the routing path. The number of all final edges is  $N_E$ . It is worth mentioning here researchers can replace Algorithm 1 with more advanced methods to check its influence on the final geolocation performance in future works.

2) *Extracting Attributes: Node Attributes*. In this work, each graph node is associated with two kinds of node attributes: node delay and node IP address. The node delay is the direct delay from the probing host to the node. For each node, the delay is repeatedly measured by the probing host many times. The minimum one is selected as the node delay because it contains minimum congestion and is closer to the true propagation delay [2]. In the end, we combine the node IDs and node attributes as the initial feature of a node.  $\mathbf{v}_i$  denotes the initial features of node  $v_i$  and  $\mathbf{V}$  denotes the initial features of all nodes.

**Edge Attributes**. Each edge can be associated with several kinds of features such as the edge delay, the head node IP address, and the tail node IP address. Here, the node nearer the probing host is called the head node of the edge, and the other one is the tail node. The edge delay is calculated by subtracting the node delay of the head node from the tail node. We keep edge delay even if it could be a negative value. Since we do not need to refine the edge representation in the GC layers, we do not need edge IDs to differentiate edges. The initial features of an edge only consist of its edge attributes.  $\mathbf{e}_j$  denotes the initial features of edge  $e_j$  and  $\mathbf{E}$  denotes the initial features of all edges.

**Algorithm 1:** Map Anonymous Routers to IP addresses

---

**Input:** Raw path set  $P_r$ , Completed path set  $P_c = \emptyset$ , Flag  $flg = 1$

**Output:** Completed path set  $P_c$

```

1 : Pick a raw path  $P_r^i$  from  $P_r$ ;
2 Add  $P_r^0$  into  $P_c$ ;
3 for each  $P_r^i \in P_r$  do
4    $flg = 1$ ;
5   for each  $P_c^j \in P_c$  do
6     if the hop count of  $P_r^i$  equals  $P_c^j$  then
7       if the hop of  $P_r^i$  equals  $P_c^j$  except
         anonymous routers then
8         Map anonymous routers in  $P_c^j$  to
           corresponding IP in  $P_r^i$ ;
9         Update  $P_r^i$  in  $P_c$ ;
10         $flg = 0$ ;
11      end
12    end
13  end
14  if  $flg = 0$  then
15    Add  $P_r^i$  into  $P_c$ ;
16     $flg = 1$ ;
17  end
18 end
19 final;
20 return  $P_c$ 

```

---

**B. The Encoder**

The encoder aims to form initial low dimensional embeddings of graph nodes and edges for the GC layers. The embeddings of graph nodes and edges are generated from the initial node features  $\mathbf{V}$  and the initial edge features  $\mathbf{E}$  from the preprocessor.

For each non-zero feature in  $\mathbf{V}$  and  $\mathbf{E}$ , we associate it with an embedding vector. Then we could get a set of low dimensional embeddings for graph nodes and edges, respectively. We concatenate the embeddings of a node (or edge) into a vector to describe the node (or edge). To be specific, the low dimensional embeddings of a node  $v_i$  and an edge  $e_j$  are:

$$\mathbf{h}_{v_i}^{(0)} = \mathbf{Q}_v^T \mathbf{v}_i, \quad (9)$$

$$\mathbf{h}_{e_j} = \mathbf{Q}_e^T \mathbf{e}_j, \quad (10)$$

where  $\mathbf{Q}_v \in \mathbb{R}^{N_v \times G}$  denotes the embedding matrix for all nodes  $V$ ,  $\mathbf{Q}_e \in \mathbb{R}^{N_e \times K}$  denotes the embedding matrix for all edges  $E$ .  $N_v$  denotes the number of node features and  $G$  denotes the embedding size.  $N_e$  denotes the number of edge features and  $K$  denotes the embedding size. The encoder then feeds  $\mathbf{h}_V^{(0)}$  and  $\mathbf{h}_E$  into the next component – the GC layers for embedding augmentation. It is worth reporting that pooling mechanisms could be applied here instead of concatenating, like average pooling, max pooling, attention-based pooling [34]. However, average pooling and max-pooling tried in our early experiments did not improve the performances. This may be because they lost some information useful for geolocation. The attention-based pooling requires more parameters which

could lead to overfitting and thus is neglected in this work. In the end, we decide to leverage concatenating to generate the feature vector.

**C. Graph Convolutional (GC) Layers**

This is the core component of the GCN-Geo system. The inputs are the initial low dimensional embeddings of graph nodes  $\mathbf{h}_V^{(0)}$  and edges  $\mathbf{h}_E$ . Its aim is to augment initial graph node embeddings  $\mathbf{h}_V^{(0)}$  by explicitly modeling the edges between nodes and graph/edge attributes. The final graph node embeddings will be sent to the decoder for location estimation. GCN is a general framework. As we mentioned in Section 3-B, GC layer consists of message, aggregate and update functions. We need to design and implement message, aggregate and update functions that are suitable for IP geolocation task.

**Message Function.** For a node  $v_i$  and one of its neighbour node  $v_j$ , the message from  $v_j$  to  $v_i$  is defined as:

$$\mathbf{m}_{i \leftarrow j} = f_{\text{message}}(\mathbf{h}_{v_j}, \mathbf{e}_{ij}), \quad (11)$$

where  $\mathbf{m}_{i \leftarrow j}$  is the message of  $v_j$  sends to  $v_i$ , and  $f_{\text{message}}$  is the message function. The inputs of  $f_{\text{message}}$  are: (i) the embeddings of the neighbour node  $\mathbf{h}_{v_j}$ ; (ii) the embedding of the edge  $\mathbf{e}_{ij}$  between the two nodes. In this paper,  $f_{\text{message}}$  is implemented as:

$$\mathbf{m}_{i \leftarrow j} = f_{\text{edge}}(\mathbf{h}_{e_j}) \mathbf{h}_{v_j}, \quad (12)$$

where  $f_{\text{edge}}$  is a two-layer MLP, which transforms the edge embedding  $\mathbf{e}_{ij}$  (size  $K$ ) to a  $G \times G$  matrix. The matrix is used as a weight to control the influence of the neighbor's message  $\mathbf{h}_{v_j}$ . The edge embedding  $\mathbf{h}_{e_j}$  is generated from the edge attributes like the edge delay and the IP addresses of two edge nodes.  $\mathbf{h}_{v_j}$  contains the node ID and attributes (e.g., IP addresses, the delay to the probing host). It is reasonable to use the transformed edge embeddings as message weight. For example, if the edge delay is too large, it may reflect that  $v_j$  is too far away, then its message is not so important to  $v_i$ ; Or if the two IP addresses are very similar, it may reflect that the two nodes belong to one organization, then  $v_i$  should pay more attention to  $v_j$ . In this way, node  $v_i$  will learn what is  $v_j$ 's information ( $\mathbf{h}_{v_j}$ ), and can decide how much information it want to receive from the relationship ( $f_{\text{edge}}(\mathbf{h}_{e_j})$ ). Here we use a two-layer MLP to learn how to control the message weights. We also leverage the activation function of ReLU [35] to catch the non-linear relationships.

**Aggregation and Update Function.**  $U_{v_i}$  denotes the set of neighbor nodes of  $v_i$ . The aggregation function  $f_{\text{aggregate}}$  collects all the messages propagated from  $U_{v_i}$  to  $v_i$ . The update function  $f_{\text{update}}$  uses the collected messages  $A_{v_i}$  to update the embedding of  $v_i$ . The aggregation and update function for  $v_i$  are defined as:

$$A_{v_i} = f_{\text{aggregate}_{v_j \in U_{v_i}}}(\mathbf{m}_{i \leftarrow j}), \quad (13)$$

$$\mathbf{h}_{v_i}^{(l)} = f_{\text{update}}(\mathbf{h}_{v_i}^{(l-1)}, A_{v_i}), \quad (14)$$

where  $\mathbf{h}_{v_i}^{(l)}$  denotes the updated embedding of node  $v_i$  after the  $l$ -th GC layer ( $l = 1, 2, 3, 4, \dots$ ).  $\mathbf{h}_{v_i}^{(0)}$  is the initial node embedding from the encoder, as shown in Formula 9. The

aggregation function  $f_{aggregate}$  can be a simply symmetric function such as Mean [11], Max [36], or Sum [37]. The Mean aggregator uses the average of all neighbors' messages as the aggregated message. The Max aggregator selects the largest value in all neighbors' messages to represent the aggregated message. The Sum aggregator sums up all neighbors' messages as the aggregated message. Since no previous work has tested them in IP geolocation, we tried all three kinds of aggregators in experiments. The update function is implemented as follows:

$$\mathbf{h}_{v_i}^{(l)} = \text{ReLU}(\mathbf{h}_{v_i}^{(l-1)} + A_{v_i}), \quad (15)$$

where we update the node  $v_i$  by summing up its previous embedding  $\mathbf{h}_{v_i}^{(l-1)}$  and its aggregated messages from neighbours  $A_{v_i}$ . And we use Relu to do non-linear feature transformation. This is important for feature learning since nodes and edges have rich semantic attributes in this paper. In this way, the new node embedding  $\mathbf{h}_{v_i}^{(l)}$  contains following information : (i) which nodes are its neighbours (topology nearby); (ii) its neighbours' attributes; (iii) its edges' attributes (e.g., IP address, delay); (iv) its own attributes (e.g., ID, IP address, delay). Then we stack GC layers and repeat the three basic functions for several times. By stacking  $l$  GC layers, a node is capable of receiving the messages propagated from its  $l$ -hop neighbors. For example, in the second time, when  $v_i$  gets messages from the neighbor  $v_j$ , it also can learn the messages from  $v_j$ 's neighbors, which are passed to  $v_j$  in the first time. After propagating with  $L$  layers, we obtain the final embeddings for all node  $V$ , namely  $\mathbf{h}_V^{(L)}$ . The final node embeddings are then fed into the decoder for location estimation.

#### D. The Decoder

The decoder aims to estimate the location information from the nodes' final embeddings  $\mathbf{h}_V^{(L)}$ . Specially, we need to predict two numerical values (latitude and longitude) of all nodes. For problems in other research areas, a general decoder after GC layers are several dense layers, which can map the final node embeddings to two-dimensional vectors. For example, a typical two-dense-layers decoder can be implemented as:

$$\widehat{loc} = \sigma \left( \mathbf{W}_{loc}^2 (\mathbf{W}_{loc}^1 \mathbf{h}_V^{(L)} + b_{loc}^1) + b_{loc}^2 \right), \quad (16)$$

where  $\widehat{loc} \in \mathbb{R}^{N_V \times 2}$  denotes the estimated location matrix for all nodes  $V$ . Specially, the two dimensions of  $\widehat{loc}$  are the estimated numerical values of latitude and longitude for all nodes.  $\mathbf{W}_{loc}^1$  and  $\mathbf{W}_{loc}^2$  are the weights of the two dense layers.  $b_{loc}^1$  and  $b_{loc}^2$  are biases.  $\sigma$  is the non-linear activation function to endorse nonlinearity, such as Relu in Formula 15. Then we can train GCN-Geo by comparing the ground-truth locations  $loc_{train}$  and the estimated locations  $\widehat{loc}_{train}$ .  $loc_{train}$  (or  $\widehat{loc}_{train}$ ) means the real/estimated locations of the training dataset.

However, this kind of decoder is not suitable for IP geolocation. In this way, the output can be any data in  $\mathbb{R}$ . The latitude and longitude range of the whole earth is (90S~90N, 180W~180E). Thus most output data is useless and only

increases the difficulty for optimization. Even finding a fine-grained location of targets among the whole earth is also not necessary. As mentioned in Section 1, fine-grained geolocation is on the basis of coarse-grained IP geolocation systems. Thus, we usually already know a rough location of the target before estimating its fine-grained location. Here we show a different way that can improve the performance of IP geolocation. First, we need to use two min-max scalars to transform the  $loc_{train}$  (latitude & longitude) into  $loc_{train}^t$ . The scales of transformed latitude and longitude in  $loc_{train}^t$  are both  $[0, 1]$ . Then our decoder is implemented as follows:

$$\widehat{loc}^{ts} = \text{Sigmoid}(\text{BatchNorm}(\mathbf{W}_{loc} \mathbf{h}_V^{(L)} + \mathbf{b}_{loc})), \quad (17)$$

where  $\widehat{loc}^{ts}$  is the estimated transformed location matrix for all nodes  $V$ . Sigmoid is an activation function of which output is  $[0, 1]$ . Sigmoid could become saturated if input values are too large, which makes learning even harder. BatchNorm refers to Batch Normalization [38]. Batch Normalization is applied here to ease the saturating problem of Sigmoid as well as preventing overfitting. Then we train GCN-Geo by comparing  $loc_{train}^{ts}$  and  $\widehat{loc}_{train}^{ts}$ . After training,  $\widehat{loc}$  can be scaled from  $\widehat{loc}^{ts}$  by reversely using two min-max scalars.

The scale of the two min-max scalars is actually a rough area that can cover all nodes in the training set. The core idea of our decoder is to find a rough area of the targets at first. In this work, we use the rough area of the training set as an approximation of this area. As we mentioned earlier, our decoder is based on an assumption that we could get a coarse-grained location of targets before fine-grained IP geolocation. A similar assumption can be found in previous fine-grained learning systems. For example, SLG needs to estimate the coarse-grained location before estimating the fine-grained location of a target. And since SLG maps target IP addresses to landmarks, the largest estimated area is actually limited to the area which the landmarks can cover. The main benefit of our decoder is that it eases the burden of fine-tuning parameters by introducing some prior knowledge. The experiments in section 5 show that this rule-based decoder significantly reduces the error distance and the epochs needed for the GCN-based model to converge.

#### E. Model Training

To learn model parameters, we employ the Mean Square Error (MSE) loss between  $loc_{train}$  and  $\widehat{loc}_{train}$ . In this work, we optimize the  $L_2$  regularized MSE loss as follows:

$$\text{Loss} = \sum_{i=1}^{N(v)_{train}} (loc_{train}^{ts} - \widehat{loc}_{train}^{ts})^2 + \lambda \|\Theta\|^2, \quad (18)$$

where  $N(v)_{train}$  denotes all nodes in the training dataset. And  $\Theta$  includes all the trainable model parameters of GCN-Geo. Deep learning methods usually suffer from overfitting. Besides Batch Normalization in the decoder, we also leverage  $L_2$  regularization to prevent overfitting. Note that Batch Normalization is only used in training, and must be disabled during testing.



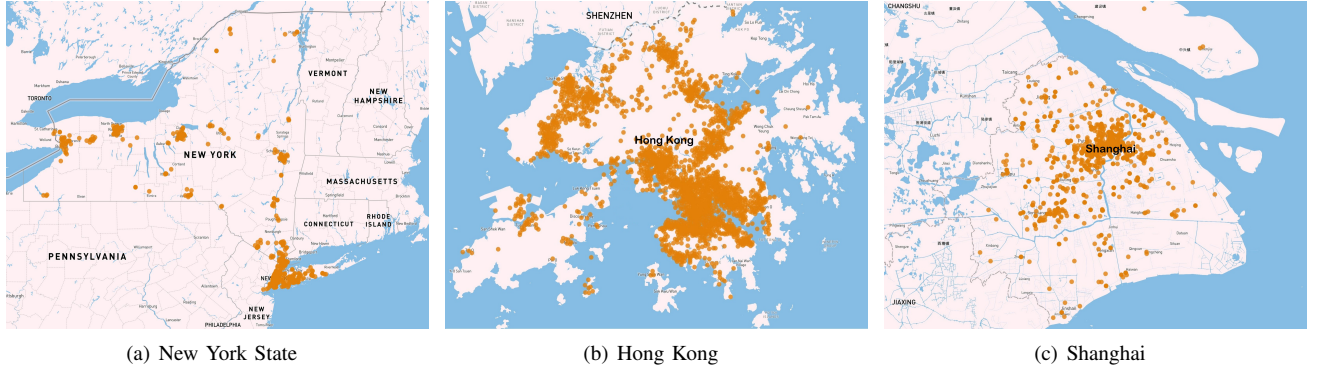


Fig. 4: Landmark Distribution of Three Areas

$\lambda$  controls the  $L_2$  regularization strength. The Adam optimizer is employed to optimize the prediction model and update the model parameters by using the gradients of the loss function.

## 5. PERFORMANCE ANALYSIS

We evaluate experiments on three real-world datasets, aiming to answer the following research questions:

- RQ1: how does GCN-Geo perform as compared with state-of-the-art rule-based and learning-based street-level IP geolocation systems?
- RQ2: how does the rule-based decoder help GCN-Geo?
- RQ3: How do different settings (e.g.,  $f_{aggregation}$ ) affect the geolocating performance of GCN-Geo?

### A. Dataset Description

To demonstrate the effectiveness and generalization capabilities of GCN-Geo, we plan to conduct experiments in various real-world networks. Due to privacy or intellectual property concerns, the datasets of most previous related works are not opened. So we need to collect our own datasets.

**Target Areas and Landmarks.** To test the generalization capabilities of GCN-Geo in different network environments, we collect landmarks from three areas: New York State (NYS), Hong Kong, and Shanghai City. In section 5, New York State is shortened as NYS, Hong Kong as HK, and Shanghai City as Shanghai. These areas belong to two continents (North America & Asia), including both developed countries and developing countries. The internet service providers (ISP) in the three areas are different. For example, the main ISPs are Spectrum and Verizon in NYS; Asia Netcom in HK; China Telecom and China Unicom in Shanghai. The size, urban environment, and terrain of these areas are also different. NYS consists of several cities and towns, including New York City, Buffalo city, Rochester city, etc. The size of NYS is  $128,897 \text{ km}^2$ . HK mainly consists of Hong Kong Island, Kowloon Peninsula, New Territories and some smaller islands. The size of HK is  $2,755 \text{ km}^2$ . Shanghai consists of the main urban area on the Changjiang alluvial plain as well as rural areas on a large island called Chongming Island. The size of Shanghai is  $6,219 \text{ km}^2$ . All these three areas cover densely populated urban areas and sparsely populated rural areas.

We collect street-level landmarks following the system in [5]. After verification and selection, there are 1705, 2061, and 1387 measurable street-level landmarks in NYS, HK and Shanghai, respectively. Each landmark is an IPv4 address with a pair of (latitude, longitude). From Fig. 4, we can see the landmark distribution in NYS, HK, and Shanghai. The latitude and longitude ranges (decimal degree) of landmarks in NYS, HK and Shanghai are (40.54N ~ 44.75N, 72.78W ~ 79.30W), (22.19N ~ 22.55N, 113.85E ~ 114.33E), and (30.71N ~ 31.65N, 121.02E ~ 121.87E), respectively. The covering area of landmarks are about in ( $467.98\text{km} \times 550.63\text{km}$ ), ( $62.50 \text{ km} \times 48.77\text{km}$ ), ( $80.49 \text{ km} \times 79.70\text{km}$ ) in NYS, HK and Shanghai, respectively. The covering area and density of landmarks also could affect the performance of IP geolocation systems [39].

### B. Engineering Applications of the Preprocessor and the Encoder

We deploy one probing host in one area. Every probing host is responsible for getting the raw traceroute data in the area where it locates. The network graph of the area is then built based on the measurement data obtained by its probing host. For 10 days, one probing host probes all landmarks in its city every 10 minutes (1440 times in total). Each probing host is a server installed with network probing tools, of which function is similar to traceroute. The software can get the IP addresses of routers between the probing host and all landmarks. And it can also obtain the delays (accurate to milliseconds) between each router and the probing host. After the preprocessor, the number of nodes (IP addresses) and the number of the links are (2872, 3303) in NYS, (3071, 3697) in HK, and (2530, 15108) in Shanghai. The edge/node ratio is 1.15, 1.20 and 5.97, respectively.

The initial attribute feature for each node is a 15-dimensional vector of values. The first 5 dimensions are the raw numerical of node delay and IP address. The numerical node delay is then binned into 10 intervals to form the last 10 dimensions. Here we use K-means to cluster delay into 10 bins. 10 is empirically selected. IP addresses can also be transformed into categorical features. The initial attribute feature for each edge is an 11-dimensional vector of values. The first dimension is the raw numerical data of the edge delay.

The remaining 10 dimensions are the binned edge delay.

Actually, it is easy to combine more kinds of features into the proposed GCN-Geo system, such as the domain name of routers, the two IP addresses of an edge, the delay changing trends of a node or edge, etc. All these features can be transformed into node/edge attribute features by the preprocessor, and then naturally introduced into model training through the encoder. And efforts can also be put into more sophisticated pre-processing techniques. For example, we can observe the histogram distribution of delay, and manually decide the number of bins for each area instead of using empirical numbers (10). IP addresses can also be explicitly transformed into categorical features. However, these features or preprocessing techniques are not easy to be applied in previous baselines for comparison. In this work, we focus on testing the learning potential of GCN in IP geolocation. Thus we utilize a simple preprocessor in this work, leaving further investigation on the preprocessor to future research.

### C. Experiments Settings

**Evaluation Metrics.** In each area, 70% landmarks are randomly chosen for training, 20% for validation, and 10% for testing (i.e., target IP addresses). We use the validation sets to do early stopping and hyper-parameters fine-tuning. We compare performances on the test sets if not specially explained. For each training set, the latitude and longitude ranges of landmarks are extended by 0.1 decimal degree, before being scaled to the  $[0, 1]$ . For example, assume the latitude and longitude range of one training set is (30.61N ~ 31.73N, 121.14E ~ 121.86E), then the range for scaling is (30.51N ~ 31.83N, 121.04E ~ 121.96E). 0.1 decimal degree is an empirical number, about 11.1 km for both longitude and latitude. We minimize the mean squared error loss following Formula 18. During the validation and test phase, we need to re-scale the output of the decoder into latitude and longitude values to calculate the geographical distance. The error distance of an IP address is the geographical distance between the ground-truth location and the estimated location. To evaluate the performance of IP geolocation, we adopt three evaluation metrics widely-used in previous works like [2, 5]: average distance error, median distance error, and max distance error. We also leverage Cumulative Distribution Function (CDF) to show the distribution of error distances.

**Parameter Settings.** We implement GCN-Geo in Pytorch. Code and hashed datasets will be opened upon acceptance. The embedding sizes of the initial node ID feature in the encoder and the hidden node representation in the GC layers are searched between  $\{32, 64, 128, 256\}$ . We optimize the model with the Adam optimizer. We leverage the default initializer of Pytorch to initialize the model parameters and embeddings. For example, standard normal distribution  $N(0, 1)$  is used to initialize node ID embeddings. A grid search is applied to find the best hyper-parameters. The learning rate is tuned amongst  $\{0.01, 0.001\}$ , the coefficient of  $L_2$  regularization is searched in  $\{0.01, 0.001, 0.0005\}$ . The depth of the GC layers  $L$  is searched in  $\{1, 2, 3, 4, 5\}$ . The number of hidden units of edge network is searched in  $\{4, 8, 16\}$ . The aggregation

methods are searched among Mean, Sum and Max. Besides, the early stopping strategy is performed: training is stopped if the average distance error on the validation set does not increase for 1000 successive epochs. Usually, 4000 epochs are sufficient for GCN-Geo to converge.

### D. Baselines

To evaluate the performance of the GCN-Geo system, we compare it with several state-of-the-art rule-based and learning-based street-level IP geolocation systems as follows.

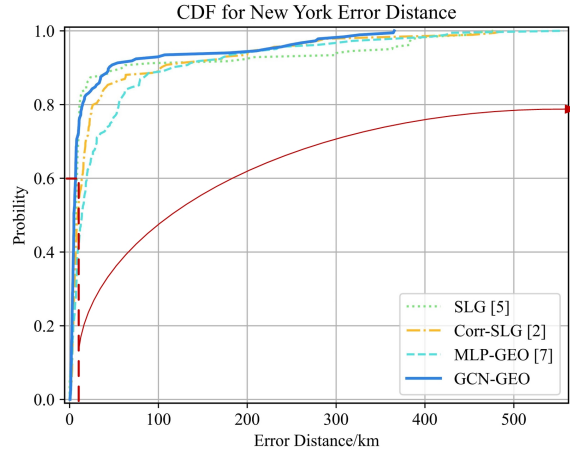
**SLG** [5]. SLG is a typical rule-based IP geolocation system and is also one of the most widely-used street-level IP geolocation baselines. Its core rule is to map a target IP to the landmark which has the smallest relative delay to the target IP. There is no need to set or tune hyper-parameters for SLG. Thus in each area, we combine the training set and validation set to geolocate the testing set.

**Corr-SLG** [2]: Corr-SLG is a recent rule-based IP geolocation system. It divides landmarks into 1) Group A, strong-positive delay-distance-correlated landmarks; 2) Group B, strong-negative delay-distance-correlated landmarks; 3) Group C, weak delay-distance-correlated landmarks. For one target, Corr-SLG selects "landmark A" with the smallest relative delay in Group A and "landmark B" with the largest relative delay in Group B. Then Corr-SLG calculates the average location of all landmarks in Group C as "landmark C". The estimated location of the target is the average location of landmark A, landmark B and landmark C. The main hyper-parameters are  $C_a$  and  $C_b$  in Corr-SLG. They are used to divide all landmarks into Group A, Group B, and Group C based on delay-distance correlation.  $C_a$  and  $C_b$  are manually tuned among  $\{0, 0.1, 0.2, \dots, 0.9\}$  and  $\{0.1, -0.2, \dots, -0.9, -1\}$ , respectively. We split the landmarks into a training set, a validation set and a testing set (same to GCN-Geo). And we use the validation set to tune  $C_a$  and  $C_b$  in each area, and then report the results on test sets. The parameter searching methods are the same as [2].

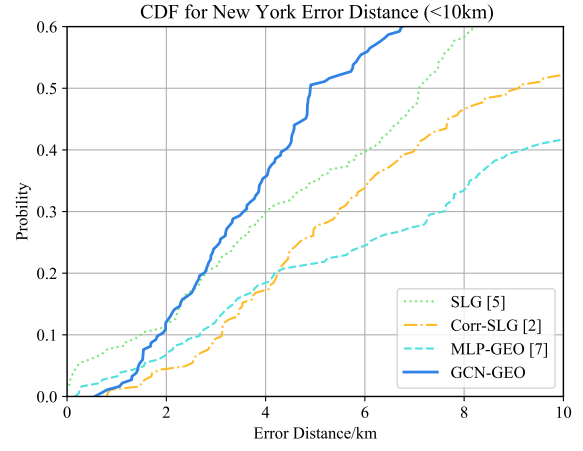
**MLP-Geo** [7]. MLP-Geo is a learning-based IP geolocation system. Like GCN-Geo and Corr-SLG, we use validation sets to tune the hyperparameters of MLP-Geo in each area. The main hyper-parameters of MLP-Geo include the learning rate, the number of training epochs and the dimension size of the middle dense layer. A grid search is applied to find the best hyper-parameters. The learning rate is tuned amongst  $\{0.1, 0.01, 0.001, 0.0001\}$ . The dimension size is searched in  $\{32, 64, 128, 256\}$ . The number of training epochs is 20,000 to find the epoch corresponding to the best performance. The other settings are kept the same as suggested in [7]. For example, we set its  $\beta$  to 30 when encoding the path.

### E. Geolocation Performance Comparison between GCN-Geo and Baselines

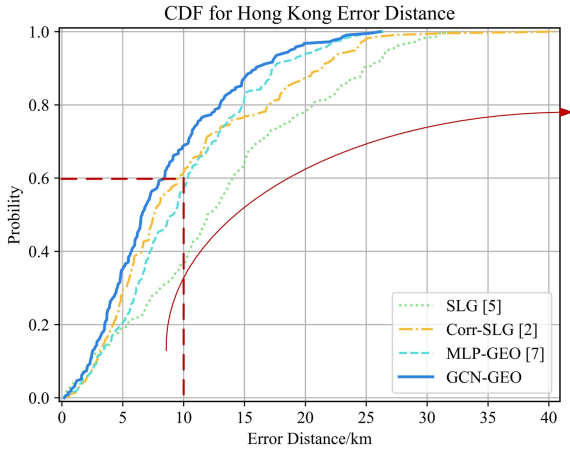
From Table I, we can see that the proposed system GCN-Geo consistently outperforms all baselines w.r.t. average error distance, median error distance and max error distance on all three datasets. Please note that we leverage MSE Loss as an optimizer target function. MSE loss aims to minimize the



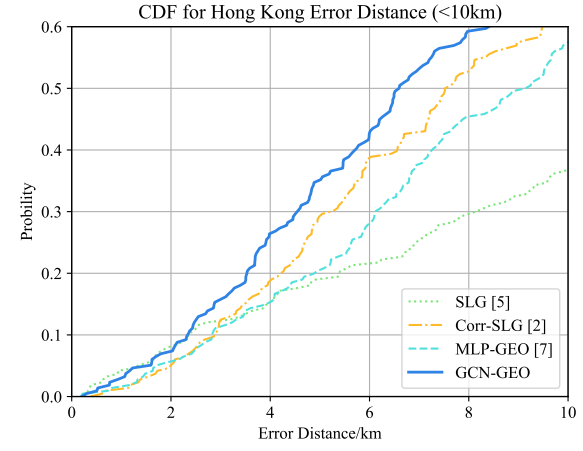
(a) New York



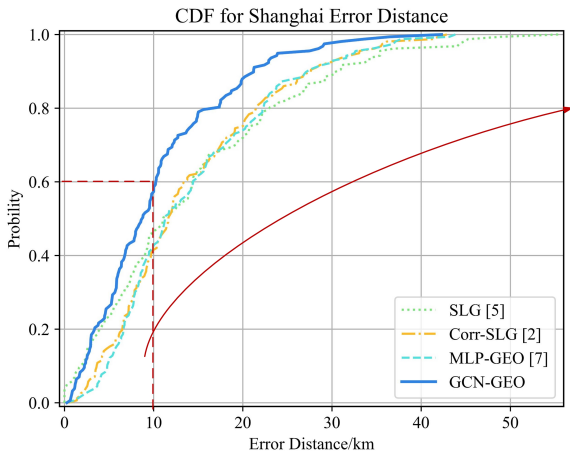
(b) New York (Error Distance &lt; 10km)



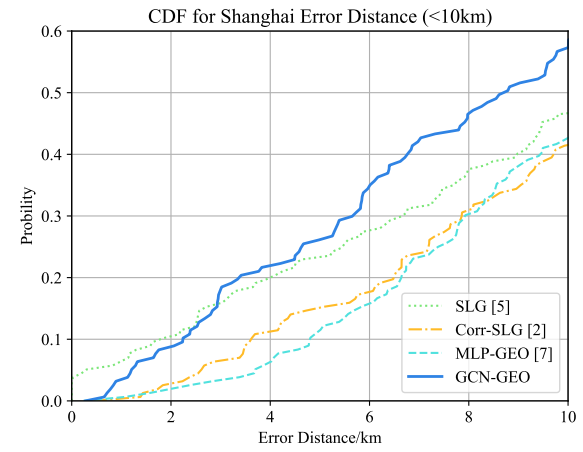
(c) Hong Kong



(d) Hong Kong (Error Distance &lt; 10km)



(e) Shanghai



(f) Shanghai (Error Distance &lt; 10km)

Fig. 5: Error Distance CDF of Three Cities (New York, Hong Kong, Shanghai)

TABLE I: Performance (kilometers) Comparison of baselines and GCN-Geo

		New York State			Hong Kong			Shanghai		
		Average	Median	Max	Average	Median	Max	Average	MEDIAN	MAX
Rule-based	SLG [5]	<b>38.176</b>	<b>7.090</b>	<b>476.861</b>	13.019	11.933	32.468	14.245	11.056	55.427
	Corr-SLG [2]	38.303	<u>7.040</u>	481.122	10.001	<u>7.523</u>	40.511	<b>14.037</b>	<b>11.281</b>	<b>42.881</b>
Learning-based	MLP-Geo [7]	43.274	13.847	<u>429.320</u>	<u>9.793</u>	<u>9.140</u>	<u>26.530</u>	14.291	11.659	43.838
	<b>GCN-Geo</b>	<b>27.198</b>	<b>4.901</b>	<b>365.528</b>	<b>8.166</b>	<b>6.596</b>	<b>26.174</b>	<b>10.368</b>	<b>8.698</b>	<b>42.292</b>
%Err Reduced		28.76%	30.38%	14.86%	16.61%	12.32%	1.34%	26.14%	21.33%	1.37%

<sup>1</sup> **bold** indicates the performance of GCN-Geo, underline indicates the best metrics among baselines, while **green colored** rows indicate the best baselines according to average error distance

<sup>2</sup> "Average" indicates average error distance, "Median" indicates median error distance while "Max" indicates max error distance.

<sup>3</sup> %Err Reduced = 100%-(best metric of baselines)/(metric of GCN-Geo)

whole loss on all data instances (not the median loss or the max loss). Thus we mainly discuss average error distance in this work. The best baseline (i.e., **green** rows) in the following sections is the baseline with the smallest average error distance on the test sets if there is no special explanation.

**Accuracy.** Compared with the best baseline (SLG) in the NYS dataset, GCN-Geo decreases by 28.76% w.r.t. average error distance; in the Hong Kong dataset (MLP-Geo), GCN-Geo decreases by 16.61% w.r.t. average error distance; in the Shanghai dataset (Corr-SLG), GCN-Geo decreases by 26.14% w.r.t. average error distance. We can see the best baselines do not always have the smallest median error distance or smallest max error distance. Compared with the smallest median error distances among baselines, GCN-Geo decreases by 30.38% in the NYS dataset (Corr-SLG); GCN-Geo decreases by 12.32% in the Hong Kong dataset (Corr-SLG); GCN-Geo decreases by 21.33% in the Shanghai dataset (SLG). Compared with the smallest max error distances among baselines, GCN-Geo decreases by 14.86% in the NYS dataset (MLP-Geo); GCN-Geo decreases by 1.34% in the Hong Kong dataset (SLG); GCN-Geo decreases by 1.37% in the Shanghai dataset (Corr-SLG). **These results clearly demonstrate that the geolocation accuracy of GCN-Geo is higher than baselines on all three metrics.** Compared with max error distance, the advantages of GCN-Geo in average error distance and median error distance area are more clear.

**Generalization. It is interesting that the best baselines are all different in the three areas.** The best baselines are SLG, MLP-Geo and Corr-SLG in the NYS, Hong Kong and Shanghai datasets, respectively. A similar pattern can be found for median error distance and max error distance, too. For median distance error, the best baselines are Corr-SLG, Corr-SLG and SLG in the NYS, HK and Shanghai datasets, respectively. For max distance error, the best baselines are MLP-Geo, MLP-Geo and Corr-SLG in the NYS, Hong Kong and Shanghai datasets. Compared with the second-best baselines, in NYS, the best baseline (SLG vs Corr-SLG) decreases by 0.33% w.r.t average error distance; the best baseline decreases (Corr-SLG vs SLG) by 0.71% w.r.t median error distance; the best baseline (MLP-Geo vs SLG) decreases by 9.87% w.r.t max error distance. Compared with the second-best baselines, in Hong Kong, the best baseline decreases (MLP-Geo vs Corr-SLG) by 2.08% w.r.t average error distance; the best baseline (Corr-SLG vs MLP-Geo) decreases by 17.69% w.r.t median error distance; the best baseline (MLP-Geo vs SLG)

decreases by 18.28% w.r.t max error distance. Compared with the second-best baselines, in Shanghai, the best baseline (Corr-SLG vs SLG) decreases by 1.46% w.r.t average error distance; the best baseline (SLG vs Corr-SLG) decreases by 1.99% w.r.t median error distance; the best baseline (Corr-SLG vs MLP-Geo) decreases by 2.18% w.r.t max error distance. From the experiments, we can see the performances of baselines are not stable in different areas. Their performance varies significantly in different network environments. For SLG, it relies on the proportion of "strong-positive-delay-distance-correlated" landmarks. For Corr-SLG, the proportion of "strong-negative-delay-distance-correlated" landmarks decides whether it can outperform SLG. **Compared with previous baselines, GCN-Geo shows better generalization capabilities in different network environments.**

#### F. An Interesting Difference between Learning-based and Rule-based systems

Fig 5 shows the cumulative probability of error distances of baselines and GCN-Geo in all three areas. In some datasets like NYS, the max error distances are too large, overlapping the smaller cumulative probability with each other. Thus we also magnify the picture (0-10 km & 0-0.6) in Fig. 5(b), 5(d) and 5(f).

From Fig. 5(a), 5(c) and 5(e), we can see that: generally, the error distances of GCN-Geo are smaller than baselines in most phases of cumulative probability. However, if we check the error distances less than 10 km, we can see SLG could be better than GCN-Geo in the beginning. For example, in Fig. 5(b), SLG is better than GCN-Geo in the smallest 11% error distances (less than 2km); in Fig. 5(f), SLG is better than GCN-Geo in the smallest 16% error distances (less than 3km). Why SLG could be better than GCN-Geo at the start and become worse in the latter part of cumulative probability?

The rule of SLG is: "the shortest delay comes from the smallest distance". Thus SLG could get very accurate geolocation results for targets that follow this rule. Some error distances could be close to 0 if the landmarks are at the same location as the targets. This is why SLG performs well in the first part of CDF. However, the disadvantage of SLG is that its error distances could be very large for targets that follow the opposite rule – "the shortest delay comes from the longest distance". The error distances of SLG are also quite large for targets of which delay has no clear linear relationship with distance. This is why the max error distances of SLG are very



TABLE II: Performance (kilometers) Comparison of Different Decoder Types

Decoder Type		New York		Hong Kong		Shanghai	
		Average	Epochs	Average	Epochs	Average	Epochs
Original	Vanilla MLP	3406.247	512	2690.566	10000	3266.079	10000
	+BatchNorm	6010.929	26	2812.680	385	1087.136	20
Rule-based	Vanilla MLP	69.663	6643	8.127	9828	12.504	3589
	+BatchNorm	29.861	2073	7.735	4690	<u>9.723</u>	1808
	+Sigmoid	<u>26.445</u>	1484	<u>7.681</u>	2265	9.843	1096
	<b>+BatchNorm+Sigmoid</b>	<b>25.165</b>	<b>3534</b>	<b>7.603</b>	<b>760</b>	<b>9.673</b>	<b>1439</b>

<sup>1</sup> **bold** actually indicates the validation average error distance of GCN-Geo, green colored underline rows indicates the best validation average error distances among other decoder types. Note all these systems only differ in decoder types.

<sup>2</sup> "Epochs" indicates the training epoch number of the corresponding results.

<sup>3</sup> These results are the best average distance errors on validation sets.

large in some datasets. So the average error distances of SLG are not so good if there are many of these kinds of targets. The cumulative probability of SLG would quickly become worse in the latter part.

GCN-Geo does not follow a specific linear delay-distance rule. Its "measurement data - location" mapping function is learned based on a supervised-learning method. The mapping function is optimized by minimizing the MSE loss of the whole training set. In other words, GCN-Geo considers the whole performance or average performance of all targets. Its mapping function tries to be suitable to as many targets as possible, instead of only focusing on a part of targets. In a dataset, if different targets follow different delay-distance or topology-distance rules, the mapping function of GCN-Geo maybe not be less accurate for some targets than SLG. This is because the mapping function needs to get better performance for other targets which do not follow linear rules. Therefore GCN-Geo can outperform SLG in the latter part of cumulative probability. Actually, we can notice that MLP-Geo follows a similar trend with GCN-Geo. In Fig. 5(d), MLP-Geo is worse than SLG before 3 km and quickly becomes better afterward. This is because MLP-Geo is also a learning-based system and is optimized by mean-square errors.

#### G. Geolocation Performance Comparison over different Decoders

As we explained in section 4-D, generally the decoders of GCN models utilize several dense layers to output the estimated latitude and longitude. However, this could be not suitable for IP geolocation tasks. Thus we propose to limit the output range first, then introduce the batch normalization layer and Sigmoid layer into the decoder. Here we compare our decoder with several baseline decoders. All these systems share the same preprocessor, encoder and GC layers. We introduce them as follows.

All decoders are divided into two groups: original and rule-based. For original decoders, they do not limit the output data range. For rule-based decoders, we scale the latitude and longitude range of the training set (+11 km) to  $[0, 1]$ . For **Vanilla MLP**, the decoder consists of a dense layer with Relu and an output layer. For **+BatchNorm**, the decoder consists of a dense layer with Relu, a batch normalization layer and an output layer. For **+Sigmoid**, the decoder consists of a

dense layer with Relu and an output layer with Sigmoid. For **+BatchNorm+Sigmoid**, the decoder consists of a dense layer with Relu, a batch normalization layer and an output layer with Sigmoid. **+BatchNorm+Sigmoid** is the decoder used in our proposed GCN-Geo system.

Table 2 shows the best geolocation performance w.r.t average error distance of all decoders on validation sets. Since these decoders share all the other components, their test performances are high likely to follow the same trend of the best performances on validation sets. So we use the performance on validation sets to compare these decoders. Note the training epochs is at most 10000 and will be early stopped if results are not improved in 1000 epochs. For each dataset, the **bold** indicates the best average error distance. "Epochs" indicate the training epoch number of the corresponding results. It can show how many epochs a decoder needs to converge.

From Table 2, we can see the best average distance errors of two original decoders are still more than 1,000 km even after 10,000 training epochs. It indicates that GCN is not a "silver bullet" to the IP geolocation problem. Though its potential in IP geolocation has been verified in Table I, simply changing its decoder could lead to unacceptable performance. The original GCN can not be directly used for IP geolocation. We still need to carefully design the structure of the whole GCN-Geo system to gain better geolocation performance.

For rule-based decoders, the performance is much better. And we can find some similar trends: 1) **+Sigmoid** and **+BatchNorm** both can clearly increase the performance and significantly reduce the epoch numbers for converging; 2) **+Sigmoid** is more accurate than **+BatchNorm** except Shanghai dataset; 3) **+Sigmoid** converges faster than **+BatchNorm**; 4) **+BatchNorm+Sigmoid** is better than only using **+BatchNorm** or **+Sigmoid**. We explain these trends as follows. Sigmoid limits the range of output into  $[0, 1]$ , which eases the burden for the optimizer. Only using Sigmoid could meet the saturating problem. Batch normalization can help to relieve the saturating problem. Batch normalization itself can also facilitate neural network training [38, 40]. Besides, it is noticed that rule-based Vanilla MLP is much better than the original Vanilla MLP, with its output still belonging to  $\mathbb{R}$ . This is because our initializers sometimes would make the decoder's estimated data in the first several epochs close to 0. If this happens, its performance could be much better than the

original MLP.

Here we want to give a short discussion of why we name the decoder as a rule-based decoder. By scaling the range of latitude and longitude to  $[0, 1]$ , we actually assume that the target IP addresses in the testing set are likely to be located at the same rough area (e.g., city or state) of the training sets. This is a typical prior knowledge thus we name the decoder as rule-based. This prior knowledge is suitable if we knew the rough city-level or state-level location of targets in advance. Actually, most fine-grained IP geolocation relies on coarse-grained IP geolocation to find the rough location at first. For example, SLG uses a classical coarse-grained IP geolocation method named CBG to find a rough area of the target at first. Then SLG uses the landmarks belonging to this area to estimate the fine-grained location of the targets. MLP-Geo also needs to cluster the landmarks and targets at first based on their measurement data, which is similar to coarse-grained IP geolocation. And it is also natural that before fine-grained IP geolocation, we use a coarse-grained IP geolocation system at first. Actually, GCN-Geo can also be used to estimate a target's coarse-grained location if we only use coarse-grained landmarks. Thus this rule may be suitable for most fine-grained IP geolocation tasks only if we can get a rough area of the targets at first. It is worth reminding here, we do not always need to scale the range of latitude and longitude of the training sets. The core idea is to find a rough area of targets, then re-scale the range of latitude and longitude of these areas to help the optimizer to converge.

These findings and the advantages of SLG shown in last section 5-F indicate that we should consider combining the advantages of rule-based and learning-based systems together to gain better performance.

#### H. The study of GCN-Geo

In this section, we investigate the impact of different learning configurations on the performance of GCN-Geo. We start by exploring the influence of the depth of the GC layers. We then study how different message aggregation methods affect the performance. The effect of Regularization Coefficients is discussed later. Finally, we analyze the influences of Graph Node Embedding Size. In Fig. 6, we show the effect of parameters on average error distance, median error distance and max error distance. However, we mainly analyze the effect of parameters on average error distance because the optimized target is MSE loss. GCN-Geo did not specifically seek a minimum median error distance or max error distance. We pick the best performance for each parameter on the testing sets. And no matter how parameters vary, the average error distances in Fig. 6 are consistently smaller than baselines in previous works for all datasets. It verifies the effectiveness of GCN-Geo, empirically showing that explicitly modeling the network connectivity can greatly facilitate the geolocation task.

1) *Effect of the Depth of the GC Layers:* The depth of the GC layers is actually the number of GC layers. From Fig. 6(a), the best layer numbers are 3, 2, 2 in NYS, HK and Shanghai, reflectively. The worst layer numbers are 1, 5, 1 in NYS, HK and Shanghai, respectively. Compared to the worst

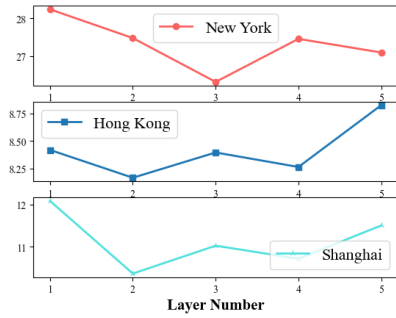
layer numbers, the improvements of the best layer numbers are 7.27% ~ 16.55%. Increasing the depth of GCN-Geo substantially enhances the geolocation performance. GCN-Geo-3 indicates GCN-Geo with three message propagation layers and similar notations for others. We can see that GCN-Geo-2, GCN-Geo-3 and GCN-Geo-4 achieve consistent improvement over GCN-Geo-1 across all datasets, which only considers the first-order neighbors only. When further stacking propagation layer on the top of GCN-Geo-4, we find that GCN-Geo-5 leads to overfitting on the Hong Kong dataset. This might be caused by applying a too deep architecture that might introduce noises to the representation learning. The marginal improvements on the other two datasets verify that conducting 2-3 propagation layers are sufficient to model the network for IP geolocation.

2) *Effect of Aggregation Methods:* From Fig. 6(d), the best aggregation methods are Max, Mean, Mean in NYS, HK and Shanghai, respectively. The worst aggregation methods are Sum, Max, Max in NYS, HK and Shanghai, respectively. Compared to the worst aggregation methods, the improvements of the best aggregation methods are 9.58%, 1.92%, 18.95%, respectively. Neighborhood aggregation is a key operation, which distinguishes GCN from MLP as we discussed in section 3-B. Theoretically, all three methods have their limitation: 1) both Mean and Sum can not treat each neighbor differently; 2) Max may only lose some neighbors' useful information. Previous work [37] has pointed out that Sum may be more powerful than Mean and Max for graphs without attributes. However, in three datasets of this paper, Mean is the best or the second-best, while Max is a little worse than Mean. Max could be the worst or the best in different datasets. The attributed graph is more complex, because the attributes of edges and nodes are also influencing the performance besides the network structure. The best aggregation methods in attributed graphs for geolocation still need more depth analysis.

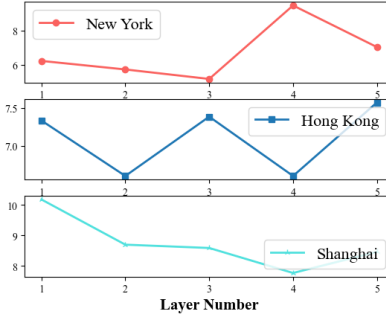
3) *Effect of Graph Node Embedding Size:* From Fig. 6(g), all the best graph node embedding sizes are 128 in NYS, HK and Shanghai. All the worst graph node embedding sizes are 256 in NYS, HK and Shanghai. Compared to the worst graph node embedding sizes, the improvements of the best graph node embedding sizes are 5.71%, 5.68%, 14.49%, respectively. The influence patterns of Graph Node Embedding Size are stable for all three datasets. Increasing embedding size brings more representation power to the GC layers by introducing more complexity. This enables the model to learn more complicated patterns. So embedding size 128 performs better than 32 and 64 in all datasets. However, a too large embedding size like 256 could disturb the model with noises and result in overfitting, especially if there are not enough data instances for training.

4) *Effect of Regularization Coefficients:* From Fig. 6(j), the best Regularization Coefficients are 0.0005, 0.001, 0.001 in NYS, HK and Shanghai, respectively. The worst Regularization Coefficients are 0.01, 0.01, 0.0005 in NYS, HK and Shanghai, respectively. Compared to the worst Regularization Coefficients, the improvements of the best Regularization Coefficients are 31.90%, 1.47%, 6.36%.  $L_2$  Regularization is the main method in GCN-Geo to overcome overfitting.

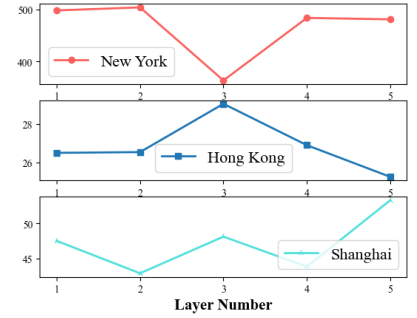




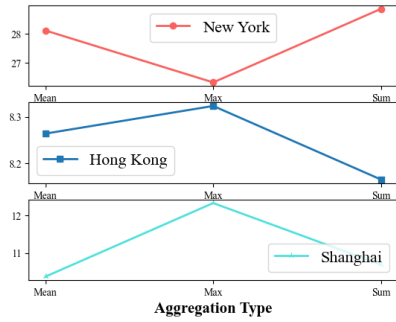
(a) Average Error(km)



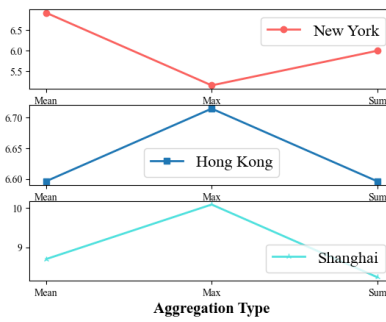
(b) Median Error(km)



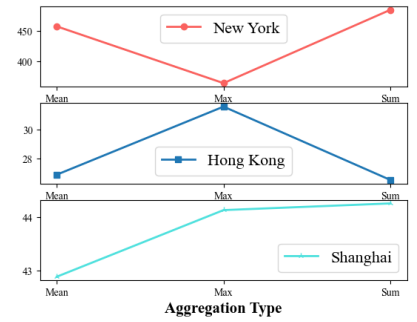
(c) Max Error(km)



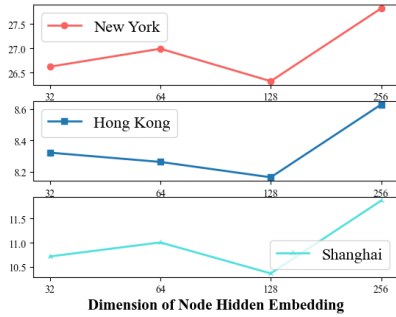
(d) Average Error(km)



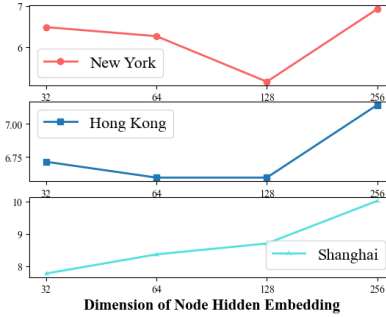
(e) Median Error(km)



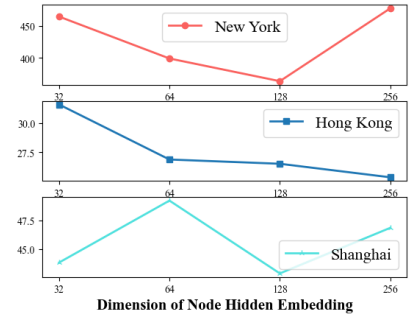
(f) Max Error(km)



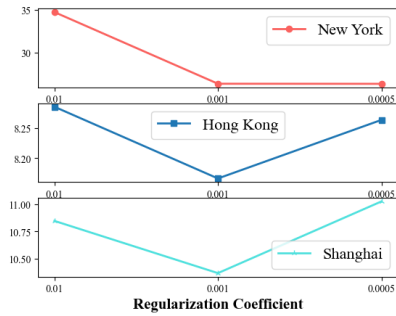
(g) Average Error(km)



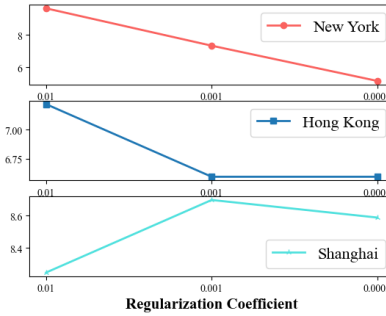
(h) Median Error(km)



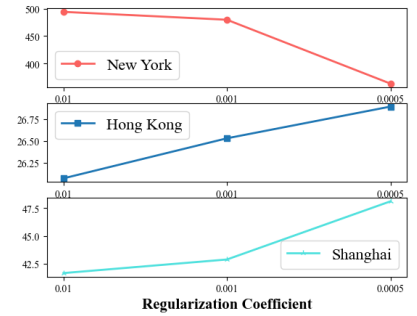
(i) Max Error(km)



(j) Average Error(km)



(k) Median Error(km)



(l) Max Error(km)

Fig. 6: Parameter Study of GCN-Geo in New York State, Hong Kong, Shanghai

However, too larger Regularization Coefficients could lead to underfitting. We find that the influence of Regularization Coefficients varies significantly in different datasets. The Regularization Coefficient is very important to NYS dataset since the improvement is larger than all the other parameters discussed in this section. However, the Regularization coefficient is the least influential parameter in the Hong Kong dataset, compared with the other parameters. Generally, the Regularization Coefficients 0.001 should be tried first because it is the best and second-best in all datasets.

## 6. CONCLUSION AND FUTURE WORK

In this work, we first formulate the measurement-based fine-grained IP geolocation task into a semi-supervised attributed-graph node-level regression problem. Subsequently, we explain the advantages of GCN (Graph Convolutional Network) compared to MLP in forming the embeddings of IP addresses. Then, we propose a GCN-based fine-grained IP geolocation system (GCN-Geo) to solve the node regression problem. The system consists of a preprocessor, an encoder, GC layers and a decoder. Moreover, we ease the converging problem of GCN-based IP geolocation systems by scaling the range of output and combining the batch normalization and Sigmoid functions into the decoder. Finally, the experiments in three different real-world datasets verify the efficiency and generalization capabilities of GCN-Geo for fine-grained IP geolocation.

The main advantages of GCN-Geo are the strong modeling ability on the computer network measurement data and the powerful extraction ability of non-linear relationships. Compared with rule-based systems, its main disadvantage is explainability, which is also a common problem for deep learning-based systems. We can clearly understand why SLG fails to map a target correctly. However, it is not easy to explain why GCN-Geo is not accurate for some specific targets. Compared with the previous deep learning-based learning system, the stronger modeling ability of GCN-Geo also needs more computing resources for training. Therefore, in future works, we still need to improve the GCN-Geo system.

We already mentioned some possible future works of the preprocessor and the encoder in section 4-A1 and 5-A. There are also other possible future works for the decoder. For example, we can consider multiple targets optimization, which aims to minimize the average, median and max error distances at the same time. The core component of GCN-Geo is the GC layers (GCN). We should think how to make the GC layers be more explainable. And the training of the GCN-Geo system is also need to be improved for large-scale industry-level IP geolocation tasks. GCN-based few-shot learning system [41] also needs to be investigated since high-quality fine-grained landmarks are hard to collect.

## REFERENCES

- [1] Q. Li, Z. Wang, D. Tan, J. Song, H. Wang, L. Sun, and J. Liu, "Geocam: An ip-based geolocation service through fine-grained and stable webcam landmarks," *IEEE/ACM Transactions on Networking*, vol. 29, no. 4, pp. 1798–1812, 2021.
- [2] S. Ding, F. Zhao, and X. Luo, "A street-level ip geolocation method based on delay-distance correlation and multilayered common routers," *Security and Communication Networks*, vol. 2021, no. 1, pp. 1–10, 2021.
- [3] Z. Wang, Q. Li, J. Song, H. Wang, and L. Sun, "Towards ip-based geolocation via fine-grained and stable webcam landmarks," in *Proceedings of The Web Conference (WWW '20)*, pp. 1422–1432, 2020.
- [4] O. Dan, V. Parikh, and B. D. Davison, "Ip geolocation using traceroute location propagation and ip range location interpolation," in *Companion Proceedings of the Web Conference (WWW '21)*, pp. 332–338, 2021.
- [5] Y. Wang, D. Burgener, M. Flores, A. Kuzmanovic, and C. Huang, "Towards street-level client-independent ip geolocation," in *9th USENIX Symposium on Networked Systems Design and Implementation (NSDI '11)*, vol. 11, pp. 27–27, 2011.
- [6] H. Liu, Y. Zhang, Y. Zhou, D. Zhang, X. Fu, and K. Ramakrishnan, "Mining checkins from location-sharing services for client-independent ip geolocation," in *IEEE Conference on Computer Communications (INFOCOM '14)*, pp. 619–627, 2014.
- [7] F. Zhang, F. Liu, and X. Luo, "Geolocation of covert communication entity on the internet for post-steganalysis," *EURASIP Journal on Image and Video Processing*, vol. 2020, no. 1, pp. 1–10, 2020.
- [8] H. Jiang, Y. Liu, and J. N. Matthews, "Ip geolocation estimation using neural networks with stable landmarks," in *IEEE Conference on Computer Communications Workshops (INFOCOM '16 WKSHPs)*, pp. 170–175, 2016.
- [9] Z. Wu, S. Pan, F. Chen, G. Long, C. Zhang, and P. S. Yu, "A comprehensive survey on graph neural networks," *IEEE Transactions on Neural Networks and Learning Systems*, vol. 32, no. 1, pp. 4–24, 2021.
- [10] V. P. Dwivedi, C. K. Joshi, T. Laurent, Y. Bengio, and X. Bresson, "Benchmarking graph neural networks," *arXiv preprint arXiv:2003.00982*, 2020.
- [11] T. N. Kipf and M. Welling, "Semi-supervised classification with graph convolutional networks," *arXiv preprint arXiv:1609.02907*, 2016.
- [12] J. Wu, X. Wang, F. Feng, X. He, L. Chen, J. Lian, and X. Xie, "Self-supervised graph learning for recommendation," in *International ACM Conference on Research and Development in Information Retrieval (SIGIR '21)*, pp. 726–735, 2021.
- [13] Y. Wu, D. Lian, S. Jin, and E. Chen, "Graph convolutional networks on user mobility heterogeneous graphs for social relationship inference," in *International Joint Conference on Artificial Intelligence (IJCAI '19)*, pp. 3898–3904, 2019.
- [14] J. Wu, W. Shi, X. Cao, J. Chen, W. Lei, F. Zhang, W. Wu, and X. He, "Disenkgat: Knowledge graph embedding with disentangled graph attention network," in *ACM International Conference on Information & Knowledge Management (CIKM '21)*, pp. 2140–2149, 2021.
- [15] J. Gilmer, S. S. Schoenholz, P. F. Riley, O. Vinyals, and G. E. Dahl, "Neural message passing for quantum chemistry," in *International conference on machine learning (ICML '17)*, pp. 1263–1272, 2017.
- [16] Y. Zhang, L. Yu, Z. Fang, N. N. Xiong, L. Zhang, and H. Tian, "An end-to-end deep learning model for robust smooth filtering identification," *Future Generation Computer Systems*, vol. 127, pp. 263–275, 2022.
- [17] C. Yin, S. Zhang, J. Wang, and N. N. Xiong, "Anomaly detection based on convolutional recurrent autoencoder for IoT time series," *IEEE Transactions on Systems, Man, and Cybernetics: Systems*, vol. 52, no. 1, pp. 112–122, 2022.
- [18] X. Wu, Y. Zhang, M. Shi, P. Li, R. Li, and N. N. Xiong, "An adaptive federated learning scheme with differential privacy preserving," *Future Generation Computer Systems*, vol. 127, pp. 362–372, 2022.
- [19] M. U. Yaseen, A. Anjum, O. Rana, and N. Antonopoulos, "Deep learning hyper-parameter optimization for video analytics in clouds," *IEEE Transactions on Systems, Man, and Cybernetics: Systems*, vol. 49, no. 1, pp. 253–264, 2019.
- [20] X. Wu, Y. Gu, J. Tao, G. Li, J. Han, and N. N. Xiong, "An effective data-driven cloud resource procurement scheme with personalized reserve prices," *IEEE Transactions on Systems, Man, and Cybernetics: Systems*, vol. 51, no. 8, pp. 4693–4705, 2021.
- [21] C. Jiang, Z. Tang, J. H. Park, and N. N. Xiong, "Matrix measure-based projective synchronization on coupled neural networks with clustering trees," *IEEE Transactions on Cybernetics*, pp. 1–13, 2021.
- [22] Y. Liu, A. Liu, N. N. Xiong, T. Wang, and W. Gui, "Content propagation for content-centric networking systems from location-based social networks," *IEEE Transactions on Systems, Man, and Cybernetics: Systems*, vol. 49, no. 10, pp. 1946–1960, 2019.
- [23] B. Abibullaev and A. Zollanvari, "A systematic deep learning model selection for p300-based brain-computer interfaces," *IEEE Transactions on Systems, Man, and Cybernetics: Systems*, pp. 1–13, 2021.
- [24] W. Jiang, "Graph-based deep learning for communication networks: A survey," *arXiv: Networking and Internet Architecture*, 2021.
- [25] A. Badia-Sampera, J. Suárez-Varela, P. Almasan, K. Rusek, P. Barlet-Ros, and A. Cabellos-Aparicio, "Towards more realistic network models

based on graph neural networks,” in *International Conference on emerging Networking Experiments and Technologies (CoNEXT '19)*, pp. 14–16, 2019.

- [26] M. F. Galmes, J. Suárez-Varela, P. Barlet-Ros, and A. Cabellos-Aparicio, “Applying graph-based deep learning to realistic network scenarios,” *arXiv: Networking and Internet Architecture*, 2020.
- [27] F. Geyer and S. Bondorf, “Deeptma: Predicting effective contention models for network calculus using graph neural networks,” in *IEEE Conference on Computer Communications (INFOCOM '19)*, pp. 1009–1017, 2019.
- [28] F. Geyer and S. Bondorf, “Graph-based deep learning for fast and tight network calculus analyses,” *IEEE Transactions on Network Science and Engineering*, vol. 8, pp. 75–88, 2021.
- [29] K. Rusek and P. Cholda, “Message-passing neural networks learn little’s law,” *IEEE Communications Letters*, vol. 23, no. 2, pp. 274–277, 2018.
- [30] T. Mallick, M. Kiran, B. Mohammed, and P. Balaprakash, “Dynamic graph neural network for traffic forecasting in wide area networks,” in *IEEE International Conference on Big Data (Big Data '20)*, 2020.
- [31] C. Yang, Z. Zhou, H. Wen, and L. Zhou, “Mstnn: A graph learning based method for the origin-destination traffic prediction,” in *International Conference on Communications (ICC '20)*, pp. 1–6, 2020.
- [32] Z. Jianlong, H. Qu, J. Zhao, H. Dai, and D. Jiang, “Spatiotemporal graph convolutional recurrent networks for traffic matrix prediction,” in *Transactions on Emerging Telecommunications Technologies*, 2020.
- [33] J. Zhou, Z. Xu, A. M. Rush, and M. Yu, “Automating botnet detection with graph neural networks,” *arXiv: Cryptography and Security*, 2020.
- [34] X. Xin, B. Chen, X. He, D. Wang, Y. Ding, and J. Jose, “Cfm: Convolutional factorization machines for context-aware recommendation,” in *International Joint Conference on Artificial Intelligence (IJCAI '19)*, vol. 19, pp. 3926–3932, 2019.
- [35] A. F. Agarap, “Deep learning using rectified linear units (relu),” *arXiv preprint arXiv:1803.08375*, 2018.
- [36] W. L. Hamilton, R. Ying, and J. Leskovec, “Inductive representation learning on large graphs,” in *International Conference on Neural Information Processing Systems (NIPS '17)*, pp. 1025–1035, 2017.
- [37] K. Xu, W. Hu, J. Leskovec, and S. Jegelka, “How powerful are graph neural networks?,” *arXiv preprint arXiv:1810.00826*, 2018.
- [38] S. Ioffe and C. Szegedy, “Batch normalization: Accelerating deep network training by reducing internal covariate shift,” in *International conference on machine learning (ICML '15)*, pp. 448–456, 2015.
- [39] G. Ciavarrini, M. S. Greco, and A. Vecchio, “Geolocation of internet hosts: Accuracy limits through cramer-rao lower bound,” *Computer Networks*, vol. 135, pp. 70–80, 2018.
- [40] S. Santurkar, D. Tsipras, A. Ilyas, and A. Madry, “How does batch normalization help optimization?,” in *International conference on neural information processing systems (NIPS '18)*, pp. 2488–2498, 2018.
- [41] L. Yang, Y. Li, J. Wang, and N. N. Xiong, “Fslm: An intelligent few-shot learning model based on siamese networks for iot technology,” *IEEE Internet of Things Journal*, vol. 8, no. 12, pp. 9717–9729, 2021.



**Shichang Ding** received the Ph.D. degree from University of Göttingen, Germany, in 2020. He is currently a lecturer at State Key Laboratory of Mathematical Engineering and Advanced Computing. His research interests include cyberspace surveying and mapping, graph deep learning, and social computing.



**Xiangyang Luo** received the Ph.D. degree from Information Engineering University, China, in 2010. He is currently a Professor and a Ph.D. Supervisor with State Key Laboratory of Mathematical Engineering and Advanced Computing. He has authored or coauthored more than 150 refereed international journal and conference papers. His research interests include multimedia security and cyberspace surveying and mapping.



**Jinwei Wang** received the Ph.D. degree in information security from the Nanjing University of Science and Technology, China, in 2007. He is currently a Professor with the Nanjing University of Information Science and Technology. He has published over 50 papers. His research interests include multimedia copyright protection, multimedia forensics, multimedia encryption, and data authentication.



**Neal Naixue Xiong** received the Ph.D. degree from the Japan Advanced Institute of Science and Technology, Japan, in 2008. He is currently a Professor in the Department of Mathematics and Computer Science at Northeastern State University, USA. He has published over 100 international journal articles and over 100 international conference articles. His research interests include cloud computing, business networks, security and dependability, parallel and distributed computing, and optimization theory.